Numerical investigation of edge flame propagation behaviour in an igniting turbulent planar jet

H. Hesse[1], N. Chakraborty[1], E. Mastorakos[2]

[1]Engineering Department, University of Liverpool,
Brownlow Hill, Liverpool, L69 3GH, United Kingdom

[2]Engineering Department, University of Cambridge,
Trumpington Street, Cambridge, CB2 1PZ, United Kingdom

1 Introduction

Many engineering applications, such as the Direct Injection (DI) engines and the relight of gas turbines in high altitudes, involve localised forced ignition of imperfectly mixed reactants. It has been found that the resulting flame from localised forced ignition in inhomogeneous reactants exhibits edge flame structure [1,2], where premixed flames are formed on both the fuel-rich and fuel-lean sides and the edge between these two branches propagate on the stoichiometric mixture fraction isosurface. The speed at which the fuel mass fraction isosurface at the edge moves normal to itself relative to an initially coincident material surface is known as the edge flame displacement speed [1,2], which is important for understanding the propagation characteristics of partially premixed flames [3]. Several previous experimental [3,4] and Direct Numerical Simulation (DNS) [1,2,5-8] studies addressed different aspects of the edge flame propagation. However, previous DNS studies [1,2] on edge flame propagation in the context of localised ignition of turbulent inhomogeneous mixtures were carried out in planar mixing layers without any mean flow and in the absence of any mean shear rate. To account for some of the above limitations, here the edge flame propagation has been analysed in terms of density-weighted edge flame displacement speed S_d^* statistics for an igniting turbulent co-flowing planar jet using 3D compressible DNS data. The above information plays an important role in modelling the propagation of turbulent edge flames [3,9].

2 Mathematical background and Numerical implementation

An igniting turbulent planar co-flowing jet is simulated using 3D DNS. The fuel-rich jet is injected through a rectangular slot into the fuel-lean co-flow. The initial mean velocity is given by [8]:

$$U(y) = (U_j + U_c)/2 + [(U_j - U_c)/2]\tanh[-(|y - y_c| - H/2)/(2\delta_0)] \quad (1)$$

where U_c =10S_L is the co-flow velocity, U_j =20S_L is the jet centre-line velocity and S_L is the laminar burning velocity of the stoichiometric mixture. In eq. 1, y_c is the distance to the jet centre-line; H is the slot height and δ_0 is the characteristic initial shear layer thickness. Following Pantano [8], δ_0 is taken to be 0.05H. The initial mean mixture fraction field is given by the following profile [8]:

Correspondence to: n.chakraborty@liverpool.ac.uk

$$\overline{\xi}(y)=\begin{cases}\xi_1\left[(1+\xi_s)/2+\left[(1-\xi_s)/2\right]\tanh\left[-\left(|y-y_c|-H/2\right)/(2\delta_0)\right]\right]+\xi_2, & |y-y_c|<H/2\\ \xi_1\left[\xi_s/2+\left[\xi_s/2\right]\tanh\left[-\left(|y-y_c|-H/2\right)/(2\delta_0)\right]\right]+\xi_2, & |y-y_c|>H/2\end{cases} \quad (2)$$

where ξ_s =0.5, ξ_1 =0.05 and ξ_2 =0.03. Consequently, the fuel and oxidiser mass fractions are initialised by: $Y_F = Y_{F\infty}\xi$ and $Y_O = Y_{O\infty}(1-\xi)$ where $Y_{F\infty}$ =1.0 and $Y_{O\infty}$ =0.233 represent the fuel and oxidiser mass fractions in pure fuel and air. The chemistry is described by a single step irreversible reaction $Fu + s.Ox \rightarrow (1+s).Pr$ where s is taken to s=4 (i.e. representative of methane/air mixture), which leads to a stoichiometric mixture fraction value equal to ξ_{st}=0.055. Although a single step chemistry is used, the activation energy and enthalpy of reaction are taken to be functions of equivalence ratio following Tarrazo *et al.* [10], which gives rise to a realistic variation of laminar burning velocity with equivalence ratio. Lewis numbers for all species are taken to be unity and $(T_{ad}-T_0)/T_0$ is taken to be 3.0 where T_0 and T_{ad} are fresh gas and adiabatic flame temperature of stoichiometric mixture. Only the thermal effects of ignition are accounted for and the details of arc formation and shock waves are not included for the sake of computational economy and the details of the localised ignition and the numerical schemes can be found in Ref. [11]. A cubic domain with side L=9H, has been used with a uniform grid of 192x192x192 nodes. The ignitor is located at the middle of the domain in the span wise direction with axial and transverse co-ordinates x=0.3H and y=0.9H from jet centreline where the Reynolds averaged value of mixture fraction is equal to ξ_{st} (i.e. $\overline{\xi}=\xi_{st}$). The boundary in the direction of jet flow is partially non-reflecting while the velocities at the jet inlet are specified by scanning a plane through a pre-computed box of frozen turbulence using Taylor's hypothesis. The inlet turbulent velocity fluctuations are modified following Pantano [8] to yield a realistic turbulent kinetic energy profile across the jet width. The transverse and span-wise boundaries are periodic. In the simulations in this paper, the rms turbulent velocity fluctuation is u'/S_L=4 and the normalized integral length scale L_{11}/l_F=3.36 where l_F is given by D_u/S_L with D_u being the unburned gas density. The density-weighted displacement speed of the edge flame is defined as [1,2]:

$$S_d^* = \rho S_d/\rho_0 = \left[\dot{w}_F - \nabla\cdot(\rho D\nabla Y_F)\right]/\left(\rho_0|\nabla Y_F|\right) = S_r^* + S_n^* + S_t^* \quad (3)$$

where S_d is the displacement speed, $\dot{w}_F$ is the fuel reaction rate magnitude and Y_F is the fuel mass fraction. The tangential strain rate $a_T = (\delta_{ij} - N_i N_j)\partial u_i/\partial x_j$ and curvature $\kappa_m = 1/2\nabla.(\nabla Y_F/|\nabla Y_F|)$ dependence of S_d^* is analysed in this study where $\vec{N} = \nabla Y_F/|\nabla Y_F|$ is the normal vector on a given Y_F isosurface. According to this convention, the local flame curvature κ_m assumes a positive value when flame surface is convex towards the unburned gas.

3 Results and Discussion

The fields of fuel mass fraction Y_F, non-dimensional temperature $T = (\hat{T}-T_0)/(T_{ad}-T_0)$, axial velocity u_1 and fuel reaction rate magnitude $\dot{w}_F$ are shown in Fig. 1 just after localised ignition (t=1.00t_{sp}), midway through the simulation (t=4.20t_{sp}) and long after the initial energy deposition (t=7.40t_{sp}). As the bulk velocity of the flow in the axial direction is greater than the flame speed, the hot gas kernel is convected away from the initial position of localised ignition. By comparing the hot region size (i.e. $T\geq$0.9) at different times, it can be seen that the flame kernel expands and the flame gets elongated towards the centre of the jet (t=7.40t_{sp}) due to the higher axial velocity there. The hot gas kernel also expands in the transverse and span-wise directions and it encloses mostly stoichiometric and fuel-rich mixtures at t=7.40t_{sp}. The simultaneous presence of high fuel concentration and high temperature due to energy deposition results in the maximum value of fuel reaction rate magnitude attained on the fuel-rich side, as evident from Fig. 1. It can also be observed from Fig. 1 that after the ignitor is switched off, the maximum temperature decreases with time and eventually settles close to the adiabatic flame temperature ($T\approx$1) ensuring self-sustained combustion. The drop in temperature causes the maximum

fuel reaction rate magnitude $\dot{w}_F$ to settle at a much smaller value a long time after the localised ignition event. The comparison between velocity magnitude and reaction rate distribution in Fig. 1 clearly suggest that the density change due to heat release significantly affects the velocity field.

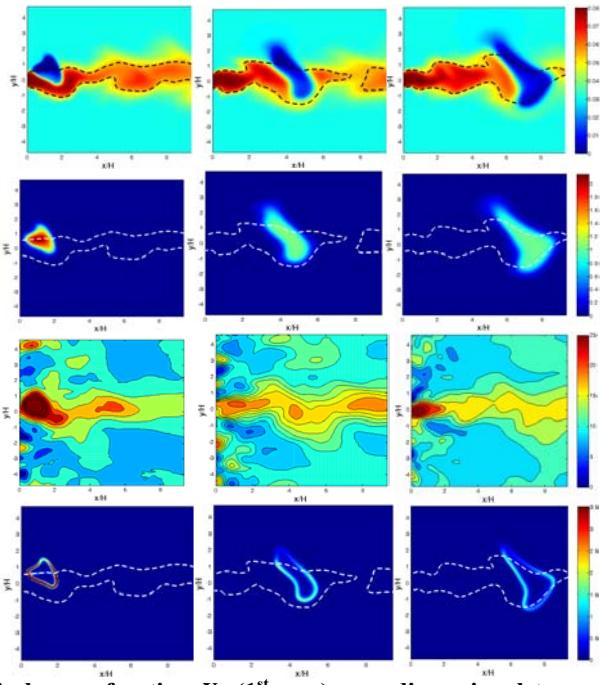

Figure 1. The fields of fuel mass fraction Y_F (1st row), non-dimensional temperature T (2nd row), axial velocity u_1 (3rd row) and fuel reaction rate magnitude $\dot{w}_F$ (4th row) at times t=1.00t_{sp} (1st column), t=4.20t_{sp} (2nd column) and t=7.40t_{sp} (3rd column). The $\xi=\xi_{st}$ isosurface is shown by black (white) broken lines on the Y_F (T and $\dot{w}_F$) fields.

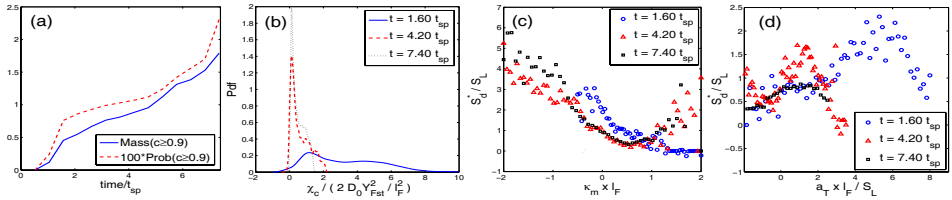

Figure 2. (a) Temporal evolution of normalised mass of burned gas region with $c \geq 0.9$ and probability of finding $c \geq 0.9$ on the $\xi=\xi_{st}$ isosurface. (b) Pdfs of χ_c in the region $0.1 \leq c \leq 0.9$ on the $\xi=\xi_{st}$ isosurface. Variation of conditional mean values of S_d^*/S_L with normalised (c) curvature κ_m and (d) tangential strain rate a_T in the region $0.1 \leq c \leq 0.9$ on the $\xi=\xi_{st}$ isosurface at different times.

The extent of chemical reaction is characterised by a reaction progress variable defined as $c=\left[(1-\xi)Y_{O\infty}-Y_O\right]/\left[(1-\xi)Y_{O\infty}-\max\left[0,(\xi_{st}-\xi)/\xi_{st}\right]Y_{O\infty}\right]$, which increases from 0 to 1 from unburned to burned gases [2]. The increase in the size of the hot gas kernel can be characterised by the temporal evolution of the mass of burned region with $c \geq 0.9$. Fig. 2a shows this mass normalised by the mass of a sphere $4\pi\delta_{th}^3\rho_0/3$ with unburned gas density ρ_0 and radius equal to thermal flame thickness $\delta_{th}=(T_{ad}-T_0)/\max\left|\nabla\hat{T}\right|$ of the stoichiometric premixed flame. It is clear from Fig. 2a that the burned gas mass increases with time indicating self-sustaining combustion. The extent of edge flame propagation on the $\xi=\xi_{st}$ isosurface is characterised by the probability of finding $c \geq 0.9$ (i.e. $P(c \geq 0.9)$) on the $\xi=\xi_{st}$ isosurface. The probability $P(c \geq 0.9)$ increases with time (Fig. 2a) suggesting that the mean edge flame speed is positive, since the burned gas area expands with time. The pdfs of

normalised cross scalar dissipation rate $\chi_c = 2D\nabla Y_F.\nabla Y_O$ for $\xi=\xi_{st}$ isosurface are shown in Fig. 2b. For premixed (non-premixed) mode of combustion χ_c assumes a positive (negative) value. It is evident that there is a finite probability of negative value of χ_c at early times, but later this probability decreases significantly and at $t = 7.40t_{sp}$ the present case exhibits a twin-flame structure with a predominantly premixed edge flame on the $\xi=\xi_{st}$ isosurface. Concerning the statistics of the edge flame displacement speed, Fig. 2c shows a predominantly negative correlation between S_d^* and κ_m although a weak positively correlating branch is evident at late times (e.g. t=7.40t_{sp}), consistent with previous findings [1-3]. The variations of S_d^* conditionally-averaged on the tangential strain rate a_T on the $\xi=\xi_{st}$ isosurface at different times are shown in Fig. 2d, which shows both positively and negatively correlating branches with a_T at earlier times (i.e. $t \leq 4.20t_{sp}$). However, the negative correlation eventually becomes negligible resulting in a positive net correlation long after the localised ignition event (e.g. t=7.40t_{sp}). The positive correlation between S_d^* and a_T is consistent with experimental data in laminar counter-flow configuration [4].

4 Conclusion

The edge flame propagation following localised forced ignition of a turbulent co-flowing planar jet has been studied in terms of density-weighted edge flame displacement speed S_d^* statistics using 3D compressible DNS data. The edge flame displacement speed S_d^* is found to be negatively correlated to κ_m; the correlation between S_d^* and a_T shows both positive and negative correlating trends but the positive correlating trend is found to be dominant at later stages of flame propagation; and the probability of finding negative S_d^* is not zero, although the mean value of S_d^* remains positive.

References

[1] Chakraborty, N., Mastorakos, E. (2006). Numerical Investigation of Edge Flame Propagation Characteristics in Turbulent Mixing Layers. *Phys. Fluids*, 18, 105103.
[2] Hesse, H. et al. (2009). The effects of the Lewis number of the Fuel on the Displacement Speed of Edge Flames in Igniting Turbulent Mixing Layers. Proc. Combust. Inst., 32:1399.
[3] Chung SH. (2007). Stabilization, propagation and instability of tribrachial triple flames. Proc. Combust. Inst. 31: 877.
[4] Mielenz, O. et al. (2000). Propagating methane/air flame in a counterflow geometry. Report ITF/LSTM/184, Institut für Thermo- und Fluiddynamik, Ruhr University, Bochum, Germany.
[5] Echekki T, Chen JH. (1998). Structure and Propagation of Methanol–Air Triple Flames. Combust. Flame 114: 231.
[6] Im HG, Chen JH. (2001). Effects of flow strain on triple flame propagation. Combust. Flame 126: 1384.
[7] Yoo C, Im HG. (2005). Transient dynamics of edge flames in a laminar nonpremixed hydrogen–air counterflow. Proc. Combust. Inst. 30: 349.
[8] Pantano C. (2004). Direct simulation of non-premixed flame extinction in a methane-air jet with reduced chemistry. J. Fluid Mech. 514: 231.
[9] Kim, J. et al. (2006). Simulation of a diffusion flame in a turbulent mixing layer by the flame hole dynamics model using level set method. Combust. Theory and Modelling. 10:219.
[10] Tarrazo, E. et al. (2006). A simple one-step chemistry model for partially premixed hydrocarbon combustion. Combust. Flame, 147:32.
[11] Chakraborty N, Mastorakos E, Cant R.S. (2007). Effects of spark ignition in homogeneous mixtures: A direct numerical simulation (DNS) study. Combust. Sci. Tech.. 179: 293.